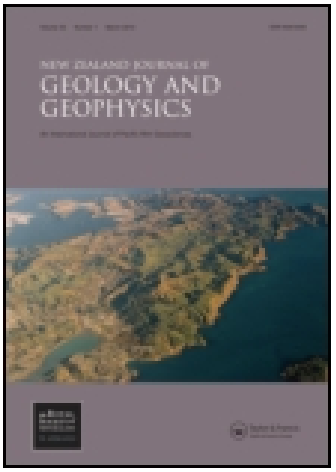

New Zealand Journal of Geology and Geophysics

Publication details, including instructions for authors and subscription information:
http://www.tandfonline.com/loi/tnzg20

Manganese deposits and the associated rocks of Northland and Auckland, New Zealand

K.J. Stanaway [a b], H.W. Kobe [a] & J. Sekula [a c]

[a] Department of Geology, University of Auckland, New Zealand

[b] 2906 Crossfork Drive, Wilmington, Delaware, 19808, U.S.A.

[c] Scott, Wilson, Kirkpatrick & Partners, Star House, Salisbury Road, Kowloon, Hong Kong

Published online: 21 Dec 2011.

To cite this article: K.J. Stanaway, H.W. Kobe & J. Sekula (1978) Manganese deposits and the associated rocks of Northland and Auckland, New Zealand, New Zealand Journal of Geology and Geophysics, 21:1, 21-32, DOI: 10.1080/00288306.1978.10420719

To link to this article: http://dx.doi.org/10.1080/00288306.1978.10420719

N.Z. Journal of Geology and Geophysics Vol. 21, No. 1 (1978): 21–32

Manganese deposits and the associated rocks of Northland and Auckland, New Zealand

K. J. STANAWAY*, H. W. KOBE, AND J. SEKULA†

Department of Geology, University of Auckland, New Zealand.

ABSTRACT

Small manganese deposits described here are associated with mafic lava, chert, and volcanic argillite and are contained in a thick sequence of indurated Permian to Jurassic eugeosynclinal sediments. Chert, volcanic argillites, and primary manganese mineralisation all result from the diagenesis and lithification of manganese and iron-enriched clay and silica sediments. These sediments precipitated out of sea water enriched with Si, Al, K, Mn, and Fe from submarine volcanic exhalations.

Primary and redeposited mineralisation bodies have been distinguished on the basis of their gross structure, microfabric relations, and relation to the present erosion surface. Microscopy of polished sections indicates that primary mineralisation contains minerals formed during sedimentation, diagenesis, deep burial, and supergene *in situ* oxidation. Redeposited mineralisation contains only supergene minerals precipitated from ground- and surface water.

The manganiferous chert, volcanic argillite, lava assemblage could, because of ubiquitous intense deformation, be derived from outside the geosyncline but could equally have appeared at the end of a eugeosynclinal sediment cycle and been subsequently deformed.

INTRODUCTION

The manganese deposits of Northland and Auckland districts are small; eleven deposits have yielded 26 000 tons with two periods of mining activity, one from 1878 to 1911 and the other from 1937 to 1960 (Reed 1960).

Extensive host rock shear and dislocation led Ferrar (1925) and Fyfe (1933) to conclude that cherts and associated manganese must have formed by replacement of sandstones and argillites in fault zones. Macpherson (1941), however, finding no evidence of replacement of sandstone by manganese mineralisation, suggested that these deposits must have formed in swamps and lakes on an ancient land surface. Intimate association of cherts and manganese led Reed (1960) to regard the deposits as resulting from submarine volcanism.

METHODS OF STUDY

Field studies involved mapping and sampling the manganese deposits and their host rocks. The regional stratigraphy for these rocks is given in Schofield 1974.

Laboratory studies included petrographic and chemical analysis of country rock types, identification of the Mn-minerals and determination of their texture by X-ray diffraction and by ore-microscopy under oil immersion. For X-ray diffraction analysis a 0·4–0·5 mg sample containing tentatively identified minerals was extracted from a polished section with a fine diamond drill and enclosed in a 0·3 mm diameter glass tube. The powder underwent FeK-radiation in a 114·6 mm diameter Debye-Scherrer camera for 70 hours.

Mn, Fe, and Si were determined by wet chemical methods and all other elements by atomic absorption and/or X-ray fluorescence.

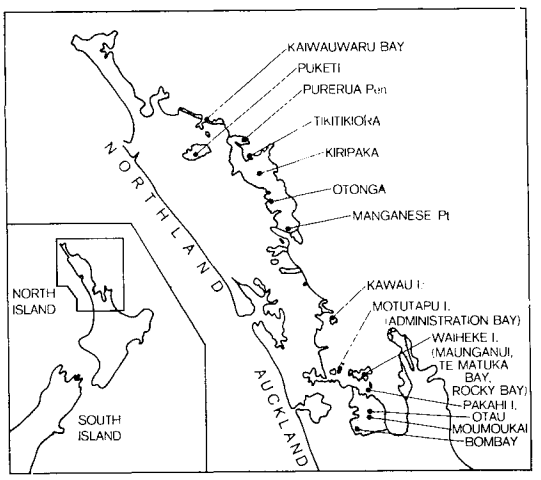

FIG. 1—Map showing outcropping Torlesse Supergroup (shaded) and some manganese deposits.

Received 27 October 1976, revised 16 August 1977.

*Present address: 2906 Crossfork Drive, Wilmington, Delaware 19808, U.S.A.

†Present address: Scott, Wilson, Kirkpatrick & Partners, Star House, Salisbury Road, Kowloon, Hong Kong.

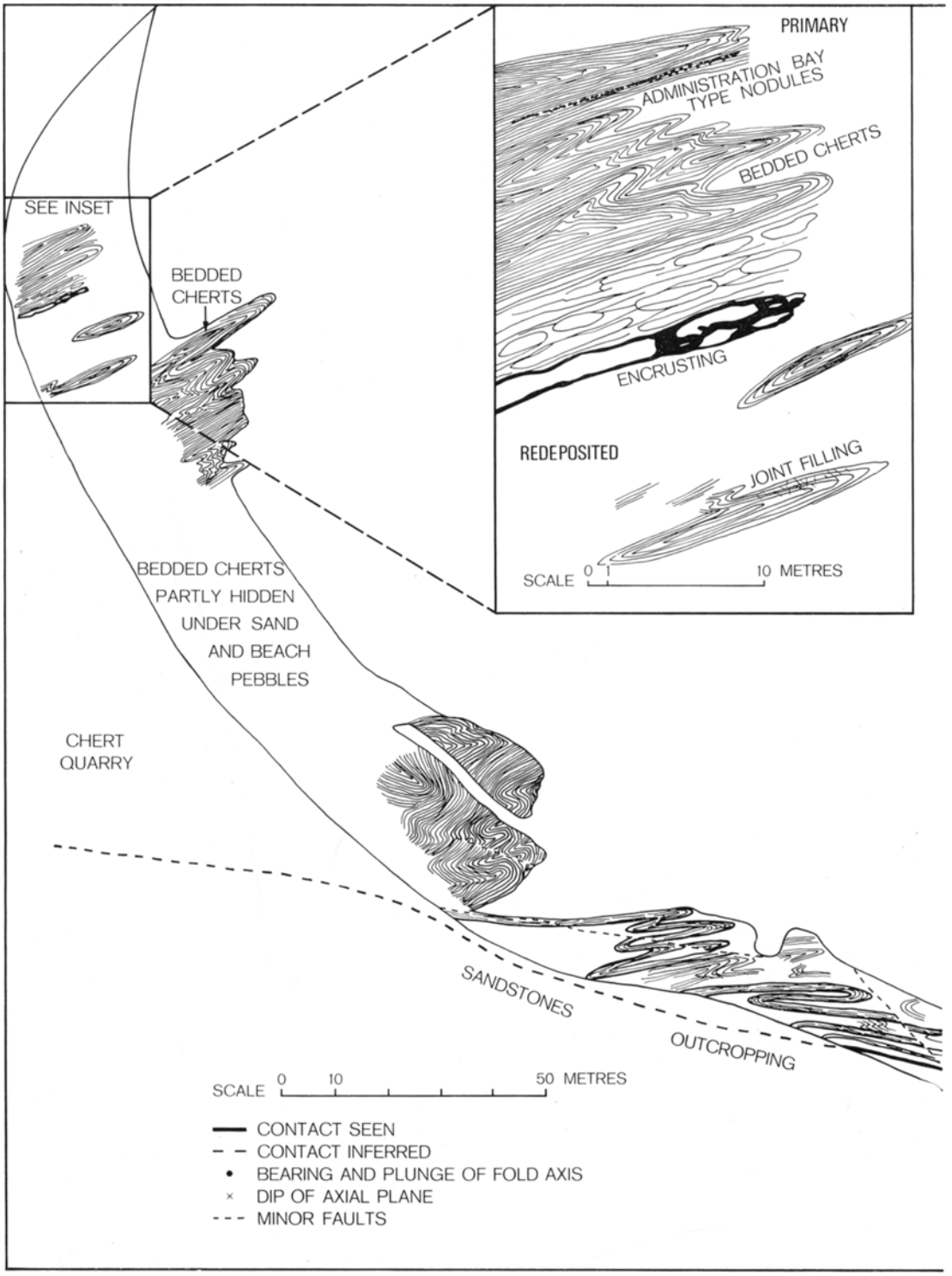

FIG. 2—Intertidal platform Administration Bay Motutapu Island showing host rock deformation and manganese mineralisation.

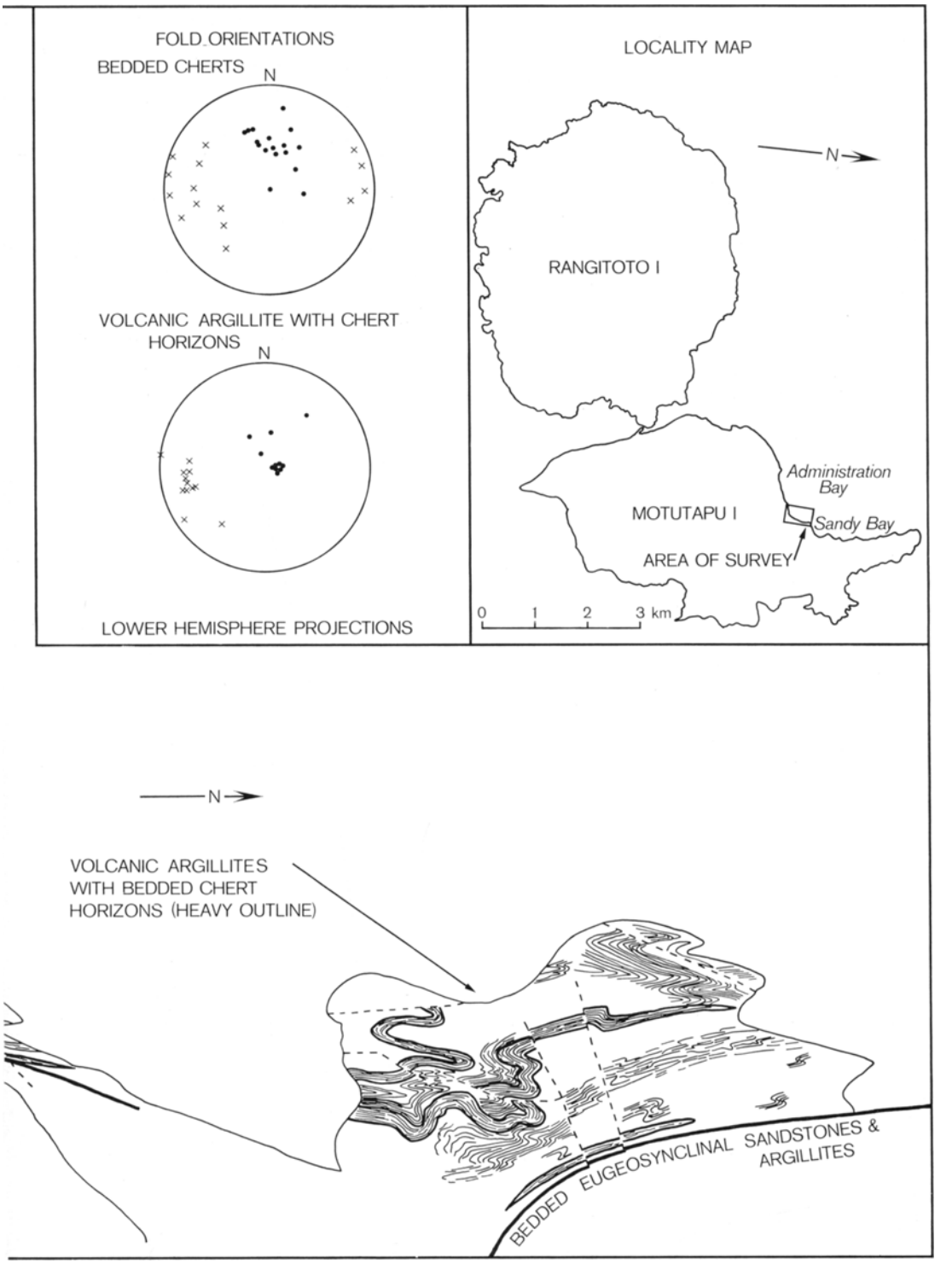

FIG. 2—*Continued*

GEOLOGICAL SETTING

The manganese deposits of Northland and Auckland are subordinate members of the volcanogenic association (see Bradshaw 1972), a rock suite which includes submarine lavas, cherts, volcanic argillites, marbles, tuffs, and rare massive sulfide lenses. The association exists as distinct lenticular units within the Torlesse Supergroup, a thick sequence of Permian to Jurassic indurated eugeosynclinal sediments which has undergone low-grade metamorphism to prehnite–pumpellyite or pumpellyite–actinolite grade (Brothers 1974; Schofield 1974; see also Fig. 1).

Most units of the volcanogenic association are only a few tens of metres thick and less than 1 km long; however, in some places they reach 1700 m in thickness and persist for up to 10 km along the regional strike.

HOST ROCKS

The most abundant sedimentary rocks of the volcanogenic association are gradational between cherts (consisting of over 90% micro/cryptocrystalline silica) and volcanic argillites (consisting of indurated clay). Lenticular 2–15 cm thick, highly siliceous beds are commonly in rhythmic alternation with much thinner less siliceous argillites. Variable amounts of disseminated manganese oxides or silicates, hematite, goethite, chlorite, calcite, sulfides, and carbon impart green, red, maroon, yellow-brown, black and grey colours. These minerals tend to concentrate more in the argillites. Accidental inclusions of radiolarian tests, silt-sized detrital grains of quartz, epidote, feldspar, and mica are scattered throughout the rocks, but frequently concentrate along some laminae.

In the field, volcanic argillites are distinguished from ordinary eugeosynclinal argillites by their colours, association with cherts or lavas, and fissile appearance. Under the microscope they show a more uniform and finer grain size (Reed 1957), indicating their origin from clay. Incipient fissility is present.

Extensive movement and dislocation have taken place within units of the volcanogenic association. Initial movement gave rise to the typical chevron and disharmonic folding seen in rhythmic chert–argillite alternations, together with the tight folding seen in some volcanic argillites (Fig. 2). Penecontemporaneous deformation and submarine slumping have left blocks of lava, chert, and sandstone embedded in foliated volcanic argillite matrix with injection of volcanic argillites into enclosing eugeosynclinal sandstones. Thick beds of greenish volcanic argillites have sometimes been mistaken for mylonite, but the presence of unbroken radiolarian tests and of lamination in less disturbed volcanic argillites indicate a sedimentary rock. Some movement, however, must have continued after sandstone and chert lithification because in a few outcrops some of the blocks are angular. Generally, blocks of lava, chert, and sandstone in volcanic argillite have some rounding and range from a few centimetres to several metres in diameter. The largest observed chert block measured 250×100×100 m, and it appears probable that much larger lava and chert bodies mapped as lenses (Schofield 1967) are also remnants of formerly more continuous horizons (see also Schofield 1974).

THE DEPOSITS

Field study of Northland and Auckland manganese deposits indicates two genetic categories with further subdivision as follows:

Primary mineralisation	large stratabound lenses lenticules, laminae and lumps "rhythmic" interlayers with chert disseminations nodules
Redeposited mineralisation	surface coatings and fracture infillings pisolites eluvials

Primary mineralisation bodies are stratabound, (Fig. 2) hard, dense, lack colloform growth layering visible to the naked eye and may reach 5 m in thickness. Minerals found include braunite, bementite, hausmannite, manganite-(a), jakobsite, ?bustamite, psilomelane, and cryptomelane; together with hematite, magnetite, chlorite, clays (illite), and quartz. Incomplete alkali metasomatism has altered some mineral assemblages to cryptomelane, and psilomelane. Supergene oxidation of primary deposits *in situ* has resulted in the replacement of some manganese minerals by nsutite, manganite-(b), and pyrolusite. Primary mineralisation, thus, has representatives from all the mineral-forming stages shown in Fig. 3.

Redeposited manganese and iron mineralisation occurs close to the present erosion surface, frequently cutting across the stratification. It can be developed spectacularly at the seashore in a strip from 1–2 m wide above the high tide mark. Other concentrations are in seasonal stream beds and soils. Redeposited occurrences all contain minerals identified as supergene (Roy 1968; Ramdohr 1969), and many display colloform growth visible to the naked eye. Psilomelane, cryptomelane, and goethite are the most common minerals, while pyrolusite, lithiophorite, nsutite, todorokite, birnessite, and manganite-(b) are also found.

Primary Mineralisation

STRATABOUND LENSES

Stratabound lenses (Fig. 4A) possess a shape similar to lenticules or micro–lenticules (Fig. 4B) and are distinguished from them solely by size. Best examples occur at Tikitikiora or in short adits on the south slopes of Maunganui, Waiheke Island. One incompletely exposed stratabound lens measured from 0·3 to 0·6 m thick by 2·3 m along the strike and extended for 3·2 m down dip. The structures closely resemble those described by Trask *et al.* (1950) from the Franciscan cherts of California, except that the Torlesse lenses are much smaller, lack adjacent massive chert, lack carbonates, and are hosted in red, rather than green rocks.

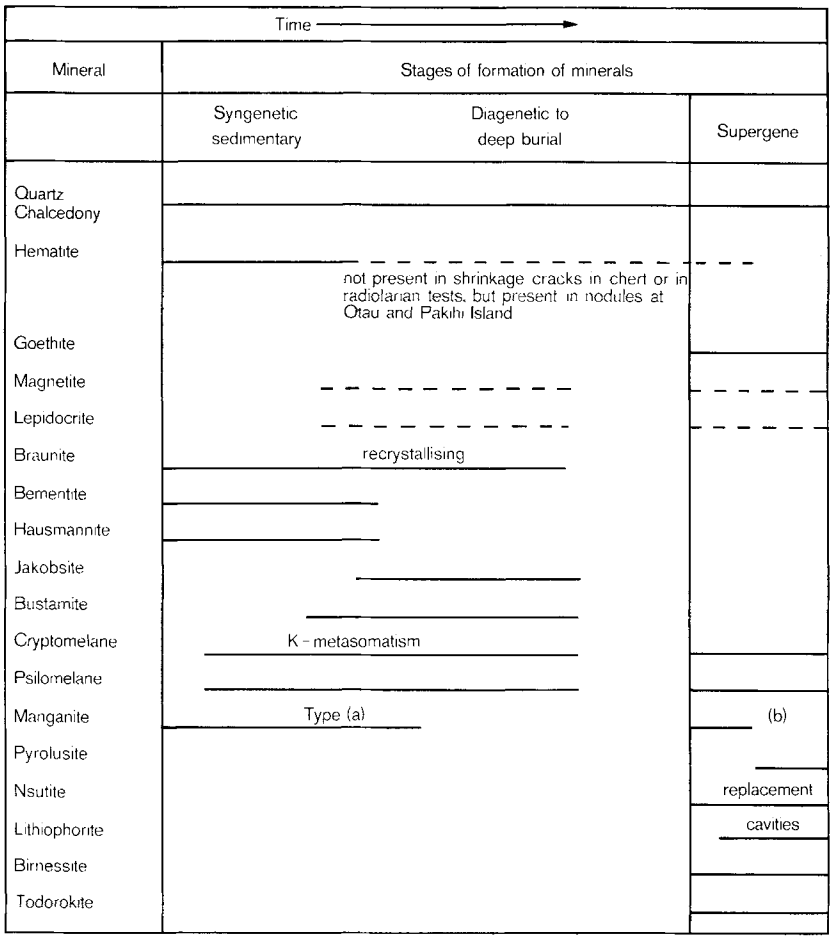

FIG. 3—Mineral paragenesis. Lines span time from beginning to ending of mineral formation. Broken lines span possible formation times for minerals whose exact paragenesis is uncertain.

LENTICULES, LAMINAE, AND LUMPS

Lenticules are discontinuous structures 1–2 cm long lining the stratification in volcanic argillites. Laminae are more continuous, some up to 20 cm long and almost 1 cm thick. Lumps can measure 10 cm or more across and form when lenticules or laminae from adjacent stratification above and below coalesce (Fig. 4B).

RHYTHMIC INTERLAYERS

Found only on the south–west slopes of Maunganui, manganiferous beds up to 1·2 cm thick alternate with beds of chert up to 6 cm thick in a manner similar to the common rhythmically alternating chert–argillite sequences. Usually the interlayered manganiferous beds are massive, but sometimes they are composed of 1 mm thick alternating argillite-manganiferous laminae (Fig. 4C). Gradation along these beds to lenticules, laminae, and lumps may also occur. Microfaulting and microbrecciation of the chert beds at mineralisation-chert contacts suggest differential compaction or bedding plane slip during folding (Fig. 4C).

DISSEMINATIONS

Disseminated mineralisation is obvious from the very dark shades exhibited by some red or white cherts and argillites, notable on Pakihi Island and south of Maunganui on Waiheke Island. Within these sequences the argillite is the more enriched member with fine manganese and iron oxide mineral grains throughout. Supergene remobilisation in all such outcrops obscures the nature of primary deposition.

NODULES

Four types of nodules are tentatively recognised as primary. The first are hard, egg-shaped nodules 3–5 mm in diameter, partly intergrown with each other. These were found at Administration Bay, Motutapu and Kaiwauwaru Bay, Northland, in red volcanic argillites as bands 3 cm wide and several metres long, parallel to the stratification (Fig. 2). A second type, found at Moumoukai as individuals or aggregates in volcanic argillites comprise soft, rounded, clay–rich nodules 1–1·5 cm in diameter. The third type found on Pakihi Island has grown from chert beds into argillite and consists of

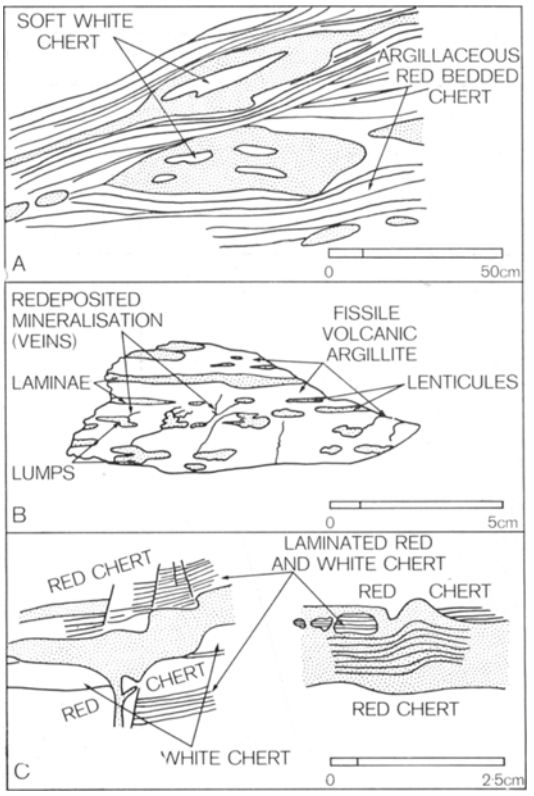

FIG. 4—Primary mineralisation types (shaded) A—Stratabound lens; B—Lenticules, laminae, and lumps; C—Interlayered with chert.

hard, coalescing knobs 1–3 cm in diameter with their surfaces cut by several sets of microfaulting or sheeting in displacements of fractions of a millimetre. The fourth type of nodule, of hematite, unspecified Mn-oxide, and clay, associates closely with manganese mineralisation at Otau. Structures of this type measure up to 10×6×3 cm and exist as coalescing aggregates, flattened parallel to the stratification of fissile volcanic argillites. Easily broken open along shear planes parallel to the fissility of the red argillites, the flat nodules display a network of open shrinkage cracks in their interior, typical of volume decrease by dehydration and solidification of a colloidal mass.

MINERALOGY AND MICROFABRIC

Along the borders of primary mineralisation bodies are oolites composed of bementite, braunite, manganite-(a), and cryptomelane. The hard, scoriaceous surfaces revealed on washing clay from some specimens of primary mineralisation (Fig. 5) is caused by aggregation of these oolites and their ragged growth into clay (Fig. 6). From the margins into the main mineral mass there are all gradations from separate oolites to compact oolite aggregates and oolites held in a manganiferous cement. These oolites usually measure between

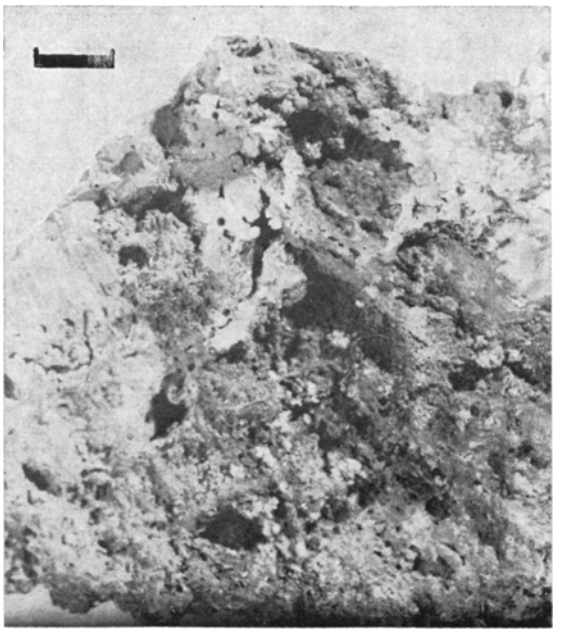

FIG. 5—Ragged surface of primary mineralisation exposed on washing away volcanic argillite matrix. White chert top right. Bar is 1·0 cm.

0·01–0·3 mm (Fig. 7), but examples 3 mm in diameter are known from one sample. Some oolites have a silica nucleus and crude growth rings characteristic of oolites (Sorem & Gunn (1967) described as "oolite-like" otherwise similar structures lacking growth rings present in manganese deposits from Olympic Peninsula).

No oolite structures were seen within the main body of lenses, lenticules or rhythmic layers. The most frequently encountered fabric consists of an irregular assemblage of braunite and cryptomelane with smaller

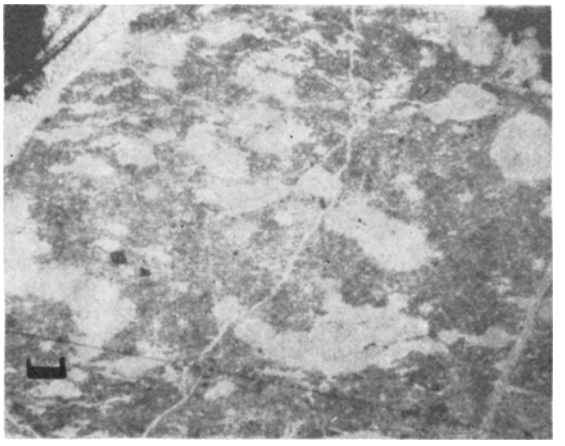

FIG. 6—Microlenticules in volcanic argillite parallelling fissility and composed of cryptomelane that has altered from braunite with redeposited (supergene) mineralisation in veinlets. Bar is 0·02 mm.

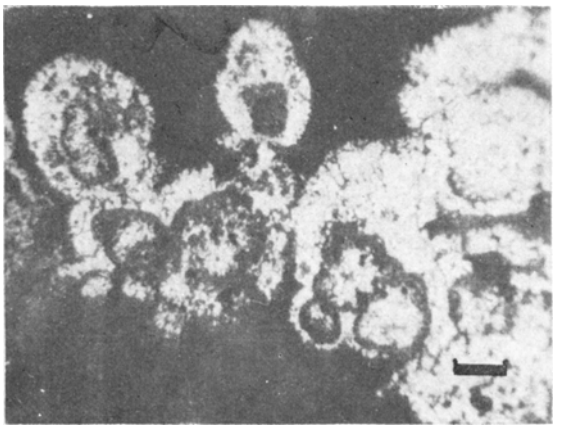

FIG. 7—Oolites within chert composed of braunite (grey) and bemenite (within oolite, but same colour as surrounding chert). Bar is 0·02 mm.

amounts of other minerals. **Braunite** forms xenomorphic and hypidiomorphic polygonal aggregates with individual crystals 5–300 μm in diameter. Interstitial **cryptomelane, manganite-(a),** clay, and quartz usually occur in cavities rimmed by the euhedral edges of braunite crystals (Fig. 8). When intergrown with other minerals, braunite exhibits the largest crystals and the greatest tendency to idiomorphic outline (Fig. 9). The cryptomelane present in primary mineralisation has a porous felted texture consisting of unoriented needles 1–50 μm long. It appears to have two positions in the paragenetic sequence existing either interstitially with braunite—implying contemporaneous crystallisation—or in irregular masses, as alteration and corrosion from braunite (Fig. 8). The latter paragenesis is evidenced from remnant braunite crystals, slight colour differences of cryptomelane masses showing up former braunite cavities, and cryptomelane extinguishing under crossed nicols in patches of similar size and shape to the

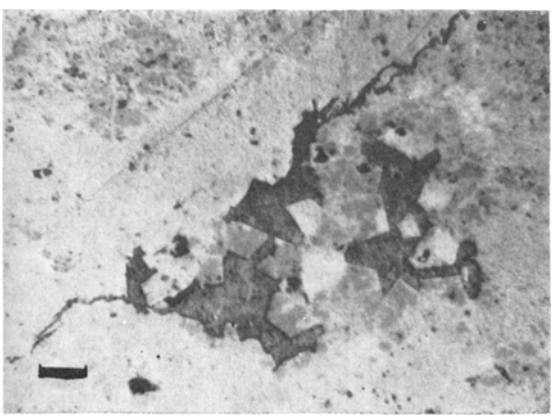

FIG. 8—Polygonal aggregate of braunite (often only grey cores) largely altered to cryptomelane (light grey) with braunite remnants now altering to nsutite (white). Prominent braunite rimmed cavity filled with clay and cryptomelane. Bar is 0·02 mm.

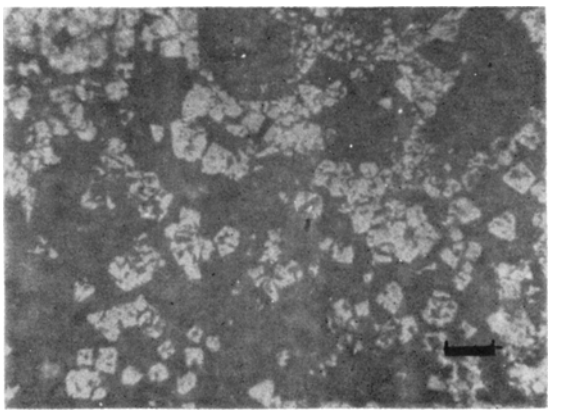

FIG. 9—Polygonal aggregate of braunite (grey) within chert (dark). Bar is 0·02 mm.

original braunite. In one specimen a few weak braunite lines appeared on an X-ray photograph of what appeared under the microscope to be merely cryptomelane. Chemical analysis shows that sometimes psilomelane rather than cryptomelane replaces the braunite.

Hausmannite occurs in a Pureru Peninsula deposit, under the microscope it appears as aggregates of fine dark grey crystals closely associated with bemenite and braunite. **Jakobsite** occurs as scattered anhedral crystals in iron-rich manganese deposits (e.g., Ruapekapeka). Identified by X-ray methods, **bementite** crystals are mostly too small to be individually visible under the microscope. Small coarser-grained patches and veinlets show yellow-brown crystals with moderate birefringence and decussate texture. X-ray data show that bementite occurs in many porous braunite crystals characterised by yellow internal reflections under reflected light.

Crystal cores rimmed by supergene alteration products and enclosed in chert are tentatively identified as **bustamite.** This mineral exhibits the following optical properties: colour, colourless; pleochroism, nil; birefringence, up to second order green; relief, greater than balsam; figure, biaxial positive with $2V = 30–35°$; extinction, straight; cleavage, in two sets at right angles in basal sections. A sample of this mineral was unobtainable for X-ray identification.

Two forms of manganite occur, both in very small amounts. The first, **manganite-(a)** is a very dark, fine-grained mineral found as sheaf-like bundles of tiny fibres, interstitial to bementite and braunite. Manganite-(b), a supergene mineral, develops in veins and as an alteration from bustamite. It is not as dark as manganite-(a) and readily alters to pyrolusite.

Supergene *in situ* oxidation of bustamite gives an assemblage of cryptomelane, nsutite, manganite-(b), and pyrolusite. Another *in situ* oxidation occurring during near-surface weathering is that of manganite to tabular subhedral **pyrolusite,** showing the typical parallel shrinkage cracks described for this alteration by Ramdohr (1969) (Fig. 10). Braunite weathers to nsutite with oxidation alteration advancing inward from crystal

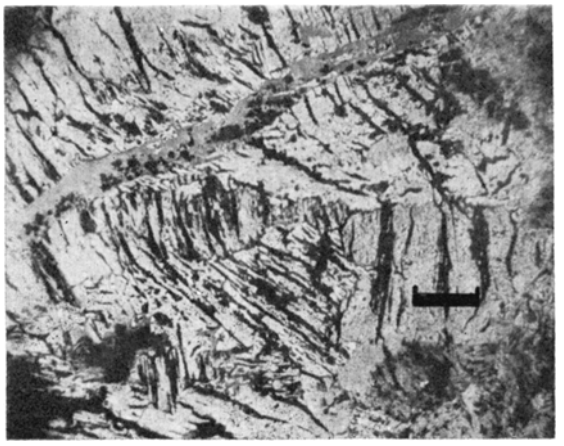

FIG. 10—Granular pyrolusite, a probably supergene alteration from manganite, showing parallel shrinkage cracks. Geothite vein (grey). Bar is 0·02 mm.

rims. One braunite crystal is usually replaced by several tabular crystals of nsutite, 2–20 μm long. Bementite and hausmannite can also alter to nsutite.

The nodules and nodular masses found in volcanic argillites consist of at least 50% clay (illite by X-ray) cemented by cryptomelane and **hematite.** In addition, X-ray analysis shows that lepidocrocite and magnetite can also be present. Shrinkage cracks ramifying through the structure have little or no clay but contain psilomelane, lithiophorite, goethite, and rare pyrolusite (Fig. 11).

Redeposited Mineralisation

SURFACE COATINGS AND FRACTURE FILLINGS

Joints filled with manganese and iron oxides appear in nearly all outcropping cherts and argillites. They are prominent on the seashore for 1–2 m above high water.

Mineralisation in large fractures and faults often shows botryoidal growth forms. Deposits found in some small seasonal streams include surface incrustations up to 30 cm thick, either as a botryoidal wad or as a hard crust cementing stream pebbles. Some encrustations may have weathered from underlying primary mineralisation (Fig. 2).

PISOLITES

A lateritic deposit with iron-manganese pisolites in the brown B soil horizon exists at Otonga over a red clay containing subrounded to subangular lumps of primary mineralisation. The deposit covers about 7000 m^2 and the underlying red clay is similar to red clays weathered from submarine lavas seen elsewhere. Pisolites can occur individually (2–5 mm diameter) or as intergrown aggregate masses 1–10 cm across. Sometimes these constitute up to 50% of the volume of the B-horizon. Concentration falls off in the yellow-brown C-horizon.

ELUVIALS

Thin deposits found near to the surface consist of lumps of manganese and iron oxides which have rolled down hill to accumulate with reworked clays in lower-lying areas.

Another type of eluvial deposit develops with the erosion of redeposited mineralisation on seashore exposures of chert and argillite. Manganese- and iron oxide-rich pebbles accumulate on intertidal platforms in sheltered bays, notably on Pakihi Island, at Te Matuka Bay on Waiheke Island, and at Manganese Point near Whangarei.

MINERALOGY AND MICROFABRIC

Microscopic features distinguishing redeposited manganese mineralisation include typical and abundant colloform growth forms (Fig. 12); well-developed veining, except in lateritic pisolites; finer crystal sizes; abundance of geothite; and large amounts of soft minerals, difficult to polish.

Indistinguishable from cryptomelane under the microscope, **psilomelane** was identified from the high barium content of remobilised mineralisation (see Table 1). Usually psilomelane and lithiophorite occur as finely intergrown crystals about 1 μm in diameter. Admixtures of these minerals with clay give grey-brown masses under the microscope, too soft to polish. Cryptomelane may also exist in these assemblages, but unfortunately there are no diagnostic X-ray diffraction lines to identify cryptomelane in the assemblages cryptomelane–psilomelane–lithiophorite, cryptomelane–lithiophorite, or psilomelane–cryptomelane. Psilomelane develops a felted texture, with component crystals sometimes in parallel arrangement. Crystals rarely grow longer than a few microns; however, where needles grow at right angles to cavity walls (comb textures) crystals can attain lengths of 50 μm.

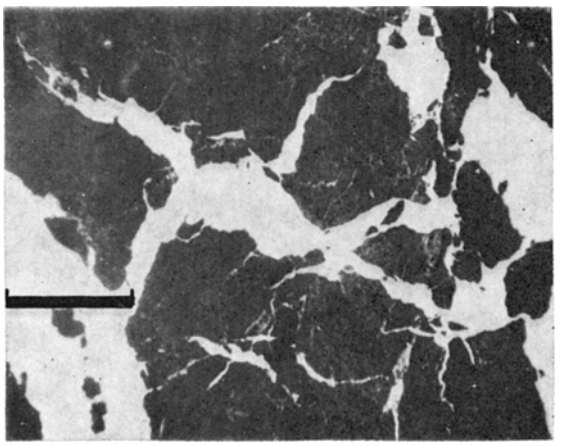

FIG. 11—Shrinkage cracks filled with psilomelane/cryptomelane (white) in nodule from Moumoukai. Main mass (too soft to polish) consists of clay, psilomelane/cryptomelane, hematite and lepidocrocite. Bar is 0·02 mm.

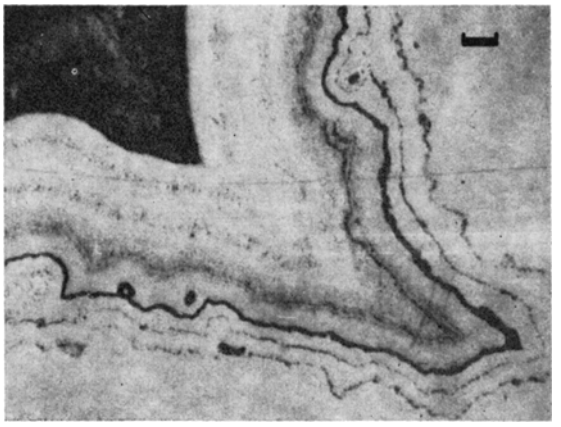

FIG. 12—Colloform growth layers consisting of cryptomelane/psilomelane (grey-white) with ?clay (thin dark bands). Soft dark mineral upper left is lithiophorite; also present in diffuse band (middle). Bar is 0·02 mm.

Lithiophorite, when unmixed with other species, is a last forming mineral in vein centres and cavity infillings (Fig. 12) and characteristically exhibits strong bireflectance (grey to blue). It grows in xenomorphic granular aggregates of crystals up to 0·01 mm in size. Goethite always appears amorphous under the microscope.

In veins, pyrolusite has a fibrous habit, with crystals oriented perpendicular to the sides of the cavity. This habit differs from that displayed when pyrolusite replaces manganite (Fig. 10). Pisolites taken from a lateritic deposit contain only goethite **todorokite,** and clay. The pisolites and pisolite aggregates possess outer layers of geothite and clay with inner cores composed of bundles of needle-shaped todorokite crystals 40–50 μm long.

Geochemistry

The element distributions shown in Table 1 relate directly to mineralogy. The Mn/Fe ratio of all but the few primary deposits containing iron minerals is above 10, while it is 10 or less for redeposited mineralisation, because of its high goethite content.

Cryptomelane formed during an early postdepositional phase of K-metasomatism, but psilomelane formed in preference to cryptomelane during near-surface weathering, probably because of a greater abundance of Ba in groundwaters.

The greater abundance of psilomelane over pyrolusite in supergene mineralisation is attributed to the strong adsorption of Ba by colloidal manganese hydroxide precipitates. Pyrolusite seems to form only from oxidation of manganite. Lithiophorite, frequently the last mineral formed in veins and cavities, reflects the presence of Li in groundwater and its high concentration in residual solutions. Anderson (1964) has shown that under supergene conditions an abundance of Cu, Pb, or Zn can give rise to crednerite, coronadite, and woodruffite respectively in preference to pyrolusite. However, the small amount of these metals in the redeposited mineralisation indicates rather a substitution of K, Ba, Mn, in the general formula (K_2,Ba,Pb) (Mn,Fe,Cu,Zn) $Mn_8^{IV}O_{16}$ given by Ramdohr (1969) for the series cryptomelane–hollandite–coronadite.

DISCUSSION

A volcanic origin for the cherts, manganese deposits, and the associated argillites is strongly favoured from their localisation and proximity to mafic submarine lavas.

TABLE 1—Partial analyses of manganese mineralisation.

Deposit	Mineralisation	%						ppm				
		MnO_2	Fe_2O_3	SiO_2	BaO	K_2O	Li_2O	Cu	Pb	Ni	Co	Sr
PRIMARY												
Moumoukai	lenticules	54.7	2.6	4.6	0.1	1.8	2.5	100	200	70	20	500
Bombay	lumps	76.0	1.0	2.0	nd	0.1	0.1	240	200	80	20	300
Bombay	lumps	43.5	1.0	1.2	nd	3.0	0.3	50	300	130	30	1000
Maunganui SW	interlayed with chert	44.7	3.8	27.2	0.6	1.3	2.5	130	200	120	20	800
Maunganui	stratabound lens	67.8	1.0	1.1	4.4	0.3	0.1	20	400	60	20	800
Pakahi Island	nodules	41.0	30.4	6.0		1.2	2.5	65	800	100	20	400
REDEPOSITED												
Pakahi	fault infilling	31.9	24.3	7.4	8.5	0.2	0.3	115	900	60	20	300
Maunganui	fault infilling	66.8	5.4	10.2	3.3	0.1	0.1	230	200	60	25	500
Rocky Bay	eluvial beach pebble	35.2	14.1	29.8	2.5	0.1	0.1	285	200	110	60	500
Otonga	lateritic pisolite	27.8	14.4	6.8	0.6	0.6	0.5	20	400	60	20	1000

nd = not detected

Analyst: T. Wilson, University of Auckland Geology Department

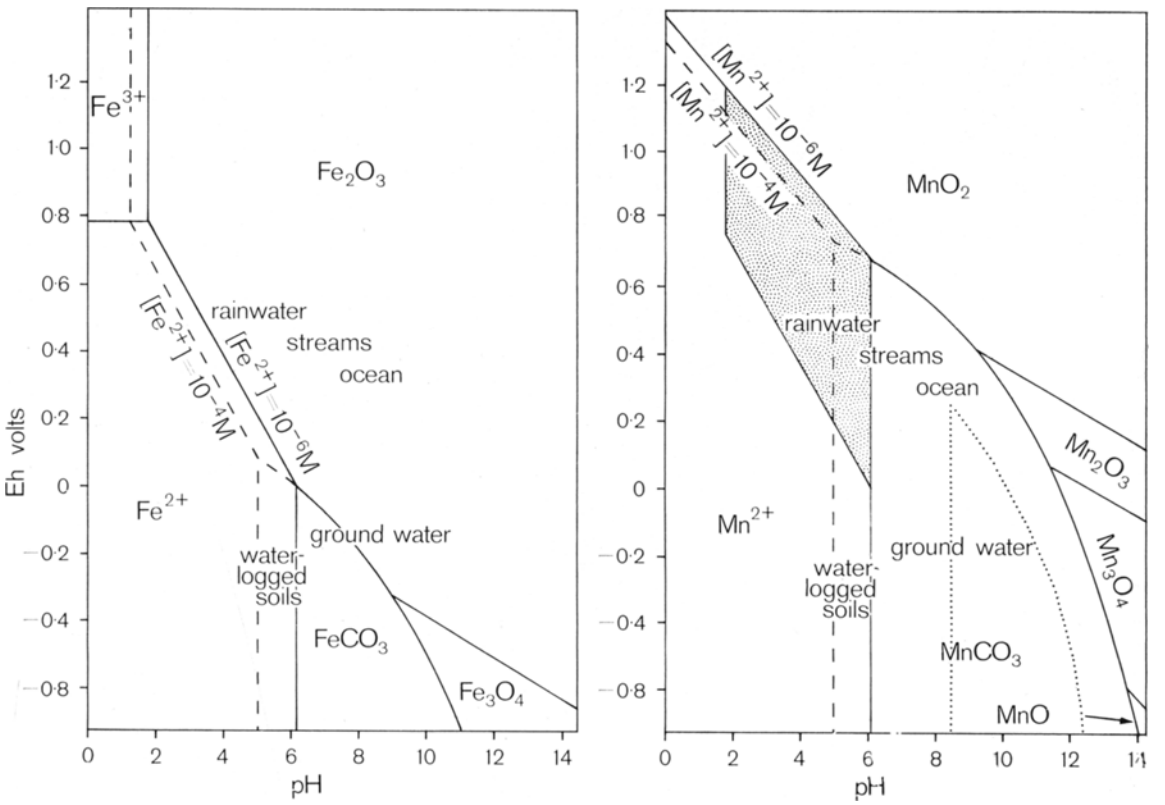

FIG. 13—Stability relations of some manganese and iron compounds in water at 25°C, 1 atmosphere total pressure, 1M carbonate concentration (from Garrels 1960 and Krauskopf 1967). Dotted line shows reduction in $MnCO_3$ field with total carbonate equal to 0·001M. Lower total carbonate will further decrease the field and increase the oxide fields.

Zelanov's (1965) investigations of the submarine volcano Banu Wuhu, which showed that fumarole activity can provide appropriate ions for the formation of the sediments found in the volcanogenic association, provides further support for this suggestion. He records sea waters charged with silica, and sea-floor precipitates comprising (by weight) 40% iron oxides, 7% manganese oxides, 0·25% titanium dioxide, up to 12% silica, 4% alumina, and 2·7% phosphorous pentoxide. About 25% by weight of the precipitates consisted of seawater salts containing Na, K, Mg, and Ca.

Silica precipitates at pH 9 when its concentration exceeds 100–140 ppm, at 25°C (Millot 1970). Water in contact with hot lavas at oceanic depths can contain over 1000 ppm of dissolved silica (Bailey *et al.* 1964). Iron and manganese concentrations can increase up to one thousand times, with potassium also increasing (Bischoff & Dickson 1975). Silica, iron, and manganese oxides can precipitate when these hot acidic waters cool and mix with ordinary seawater to become slightly alkaline and more oxidising (Fig. 13). Ordinary seawater has a temperature range from 0–30°C with a pH around 8 and an Eh around 12·5 (Sillén 1961). Alternatively, if the hot ion-charged waters boil, any ions present in the vapour phase will precipitate, probably as oxides and hydroxides following pressure decrease as the bubbles rise to the surface.

The formation of clays in ion-charged seawater arises because Al ions can induce rapid precipitation of silica. Wey & Siffert (1962) show that the solubility of an initially saturated silica solution (140 ppm at 25°C) falls to 30 ppm silica and 1 ppm alumina when 40 ppm alumina is added at a pH between 7 and 10. According to Krauskopf (1967) and Millot (1970), synthesis of clay minerals is ensured by simple reaction from dilute solutions containing appropriate ions. In Millot's scheme clays can be formed either by subtraction (acid or alkaline environments) when ions are removed until those appropriate to clay formation remain, or by addition (alkaline environment only) when appropriate ions accumulate. Clays of the volcanogenic association could form both syngenetically as ions accumulated in weakly alkaline seawater and/or diagenetically as ions accumulated in interstitial waters rich in alkaline and alkaline earth elements (cf. Zelanov 1965).

The following evidence supports the argument that volcanic argillite represents lithified siliceous clays formed during both sedimentation and diagenesis, and that only a very minor amount of clay is derived from *in situ* weathering of submarine tuffs, the devitrification of volcanic glass, and the accumulation of land-derived (deep sea) clay.

1. Corroded or remnant detritus is not found.

2. Glass shard structures are not generally found. On one outcrop shards lie preserved in thin tuffs interstratified with sandstones adjacent to thick volcanic argillites in which shards are lacking.

3. Initial deposits must have been very fine-grained, because less deformed volcanic argillites show fine lamination as colour bands. These sometimes contain different proportions of fine detritus.

4. Complete gradation from chert to volcanic argillite, with pervasive and sharply-bounded colouration, can only be caused by microscopically even dispersal of probably colloidal-sized clay, silica, hematite, and chlorite, etc.

5. The shape and ragged edges of manganiferous lenticules and microlenticules (Fig. 6) indicates growth in fissile clay (depositional fabric). Zaritskiy (1969) has shown that concretion shape is determined by medium asymmetry and not compression, and in this respect it is significant that the oolites in cherts tend to be spherical (Fig. 7).

6. Manganese mineralisation accompanying the slowly accumulating deep sea clays (0·1–1 cm per 100 years: Wedepohl 1971) grows on the sea floor as reniform crusts and nodules around objects, but mineralisation of the volcanogenic association has grown within sediment as lenses, lenticules, microlenticules, and oolites indicating rapid sedimentation and burial. Negligible trace elements of the volcanogenic association manganese deposits also implies rapid sedimentation and a limited period in contact with sea water (Table 1).

It is unlikely that volcanic argillite represents impurity oxides expelled when silica gel converts to crystalline silica (Davis 1918), because the beds of volcanic argillite are sometimes tens of metres thick, with chert and free silica only minor constituents.

Sediments of the volcanogenic association prominently display structures such as nodules, lenses, and rhythmic interlayering indicative of diagenetic unmixing of manganese-silica-clay precipitates. Some separation, however, must be syngenetic with sedimentation because in relatively undeformed volcanic argillites, colour bands (red, green, maroon) and bands of chert at least 1 m thick and continuous for over 100 m can be mapped (Fig. 2). Primary manganese mineralisation also occurs only along particular, persistent stratigraphic horizons. Only within these bands or horizons has diagenetic segregation left discontinuous structures. Figure 13 shows that there is a range of Eh–pH values (shaded area) for which manganese, but not iron, is significantly soluble. Silica also remains relatively immobile under these conditions. Thus, under appropriate conditions of Eh, pH, and manganese concentration, manganese deposits could form by migration and segregation of manganese (analogously to concretion formation in calcareous sediments) with silica immobilised and iron remaining dispersed as fine-grained hematite. Similarly, diagenetic segregation of silica from clay, iron, and manganese probably took place under more alkaline conditions since silica is more soluble above pH 9 (Krauskopf 1967). In only a few localities, notably at Otau, Kiripaka, and Pakihi, has iron segregated into nodules, either with or without manganese. From Fig. 13 this would have required a low pH–Eh environment.

Like present-day submarine nodules, initial iron-manganese precipitates were probably largely amorphous with the oolites (now visible only at mineralisation-host rock boundaries) most representative of this original material. Although these oolites could have started growth in sea water, accretion must have continued within the sediment because some oolites are up to 3 mm diameter; some growth rings enclose several oolites (Fig. 7); some oolites have asymmetric growth rings indicating immobility and competition for space (Fig. 7); oolites in volcanic argillite tend to be more lenticular than those in chert (Figs 6, 7); and larger oolites can enclose radiolarian tests.

The extent to which the minerals now seen have recrystallised or represent altered original minerals is unknown. Bementite and manganite-(a), however, probably represent little recrystallised syngenetic/diagenetic material (Fig. 3), since they appear both crystalline and cryptocrystalline and lack replacement textures. Bementite occurs within sharply defined growth layers within some oolites as also does braunite. The latter, with its large, well-formed crystals probably crystallised from original smaller less well-defined crystals (Fig. 7). This recrystallisation probably took place during diagenesis, because chert enclosing porous braunite crystals elsewhere, suggests either prior or simultaneous formation of braunite in chert (Fig. 9). Diagenetic recrystallisation has also involved metasomatic alteration of a substantial portion of the braunite (possibly also bementite and hausmannite) to cryptomelane. This alteration requires the addition of potassium, probably from waters trapped within the sediment (see Zelanov 1965). Exhaustion of this element probably accounts for the incomplete alteration since montmorillonite clays converting to illite and chlorite would have competed for the potassium (Dunoyer de Segonzac 1970). Although not found in oolites, hausmannite was considered a primary mineral because of its intimate association with bementite and because Sorem & Gunn (1967) considered it primary in the similar deposits of the Olympic Peninsula.

Quartz veining of cherts and manganese mineralisation provides evidence of continued silica mobility during deep burial, but there is no evidence of chemical mobility of manganese or iron during this period. Manganese appears to have mobilised only in response to pressure stress in fractured cherts (Fig. 4C).

Following uplift acid meteoric water and ground waters of low Eh remobilised the iron and manganese in the cherts, argillites, and lavas. Precipitation occurred again when the Fe^{2+} and the Mn^{2+} bearing solutions encountered highly oxidising and/or alkaline conditions in fractures, on surfaces, and in soils in contact with the air (Fig. 13).

ACKNOWLEDGMENTS

The authors appreciate the very generous grants made by New Zealand Steel (to Kerry J. Stanaway) and Winstones Limited (to John Sekula) enabling this study to be made. Work was done by two of the authors (KJS and JS) for M.Sc. theses at the University of Auckland. We would like to thank Drs K. B. Sporli and P. M. Black, Professor R. N. Brothers, and numerous property owners for their help in the course of our studies.

REFERENCES

ANDERSON, J. A. 1964: Geochemistry of manganese oxides, a guide to sulfide ore deposits. (Unpublished PhD. thesis, lodged in the Library, Harvard University.)

BAILEY, E. H.; IRVIN, W. P.; JONES, D. L. 1964: Franciscan and related rocks, their significance in the geology of Western California, *California Division of Mines and Geology, Bulletin 183.*

BISCHOFF, J. L.; DICKSON, F. W. 1975: Seawater–basalt interactions at 200°c and 500 bars: implications for the origin of sea floor heavy metal deposits and regulation of seawater chemistry, *Earth and Planetary Science Letters 25*: 385–97.

BRADSHAW, J. D. 1972: Stratigraphy and structure of the Torlesse Supergroup (Triassic–Jurassic) in the foothills of the Southern Alps near Hawarden (S60–61), Canterbury. *N.Z. Journal of Geology and Geophysics 15*: 71–87.

BROTHERS, R. N. 1974: Kaikoura orogeny in Northland, New Zealand. *N.Z. Journal of Geology and Geophysics 17*: 1–18.

DAVIS, E. F. 1918: The radiolarian cherts of the Franciscan Group. *University of California Bulletin II*: 235–432.

DUNOYER DE SEGONZAC, G. 1970: The transformation of clay minerals during diagenesis and low-grade metamorphism: a review. *Sedimentology 15*: 281–346.

FERRAR, H. T. 1925: The geology of the Whangarei–Bay of Islands Subdivision. *N.Z. Geological Survey Bulletin*: 27.

FYFE, H. E. 1933: Manganese deposit, Bombay. *N.Z. Journal of Science Technology 15*: 203–7.

GARRELS, R. M. 1960: "Mineral equilibria". Harper Brothers, New York. 253p.

KRAUSKOPF, K. 1967: "Introduction to geochemistry". McGraw-Hill, New York. 721p.

MACPHERSON, E. O. 1941: Manganese deposits in the Manukau and Franklyn Counties. *N.Z. Journal of Science and Technology B22*: 185–92.

MILLOT, G. 1970: "Geology of clays". Springer, Berlin, New York. 398p.

RAMDOHR, P. 1969: "The ore minerals and their intergrowth". Pergamon, Oxford. 1174 p.

REED, J. J. 1957: Petrology of the lower Mesozoic rocks of the Wellington District. *N.Z. Geological Survey Bulletin 57.*

REED, J. J. 1960: Manganese ore in New Zealand. *N.Z. Journal of Geology and Geophysics 3*: 344–54.

ROY, S. 1968: Mineralogy of the different genetic types of manganese deposits. *Economic Geology 63*: 760–86.

SCHOFIELD, J. C. 1967: Sheet 3 Auckland. "Geological Map of New Zealand 1:250 000". N.Z. Department of Scientific and Industrial Research, Wellington.

——— 1974: Stratigraphy, facies, structure and setting of the Waiheke and Manaia Hill Groups, East Auckland. *N.Z. Journal of Geology and Geophysics 17*: 807–38.

SILLÉN, L. G. 1961: The physical chemistry of seawater. Pp. 549–81 *in* SEARS, M. (Ed.): Oceanography. *American Association for the Advancement of Science Publication 67.*

SOREM, R. K.; GUNN, D. W. 1967: Mineralogy of manganese deposits, Olympic Peninsula, Washington. *Economic Geology 62*: 22–56.

TRASK, P. D.; WILSON, I. F.; SIMONS, F. S. 1950: Manganese in California; summary report. *California Division of Mines Bulletin 125*: 56–65.

WEDEPOHL, K. H. 1971: "Geochemistry". Holt, Rinehart, Winston, New York. 231p.

WEY, B.; SIFFERT, R. 1962: Synthese d'une sépiolite a temperature ordinaire. *Académie des Sciences, Comptes Rendus 254*: 1460–62.

ZARITSKIY, P. V. 1969: Reasons for flattened shapes of concretions. *Doklady Akademia Scientia SSR 188*: 177–9.

ZELANOV, K. K. 1965: Iron and manganese in exhalations of the submarine Banu Wuhu volcano (Indonesia). *Doklady Akademia Scientia SSR 155*: 94–6.